Electronic Supplementary Information (ESI)

Elastic MXenes Conductive Layers and Electrolyte Engineering Enables Robust Potassium Storage

Xinyue Xu[#], Qingqing Jiang[#], Chenyu Yang[#], Jinxi Ruan, Weifang Zhao, Houyu Wang, Xinxin Lu, Zhe Li, Yuanzhen Chen, Chaofeng Zhang*, Juncheng Hu,* Tengfei Zhou **

X. Xu, Q. Jiang, W. Zhao, Z. Li, J. Hu
Key Laboratory of Catalysis and Energy Materials Chemistry of Ministry of Education, Hubei Engineering Technology Research Centre of Energy Polymer Materials, School of Chemistry and Ma terials Science, South-Central Minzu University, Wuhan 430074, China

E-mail: qqjiang@mail.scuec.edu.cn; jchu@mail.scuec.edu.cn

C. Yang, J. Ruan, H. Wang, X. Lu, C. Zhang, T. Zhou

Institutes of Physical Science and Information Technology, Anhui University, Hefei 230601, China

E-mail: cfz@ahu.edu.cn; tengfeiz@ahu.edu.cn

Y. Chen
State Key Laboratory for Mechanical Behavior of Materials, School of Materials Science and Engineering, Xi'an Jiaotong University, Xi'an 710049, People's Republic of China.

#X. Xu, Q. Jiang and C. Yang contributes equally to this work.

1. Experimental Methods

1.1 Materials and chemicals

All reagents were readily available from commercial sources and were used as received without further purification. Cobalt nitrate hexahydrate ($Co(NO_3)_2 \cdot 6H_2O$), methyl alcohol (CH_3OH, 99%) and hydrofluoric acid (HF, 37%) were purchased from Sinopharm Chemical Reagent Co., Ltd. Dimethyl imidazole ($C_4H_6N_2$, 98%), dicyandiamide ($C_2H_4N_4$, 99%) and potassium hexafluorophosphate (KPF_6, 99%) were purchased from Aladdin Reagent. Ti_3AlC_2 powders (200 mesh) were purchased from 11 technology Co., Ltd. N-methyl pyrrolidone (NMP), polyvinylidene fluoride (PVDF, hsv900), 1,2-dimethoxyethane ($C_4H_{10}O_2$, 99.5%) were purchased from Sigma Aldrich. Potassium bis(fluorosulfonyl)imide (KFSI, > 95.0%), ethylene carbonate ($C_3H_4O_3$, 99.0%) and diethyl carbonate ($C_5H_{10}O_3$, > 98.0%) were purchased from TCI (Shanghai) Development Co., Ltd.

1.2 Synthesis of $Ti_3C_2T_x$ nanosheets

Ti_3AlC_2 powders (0.5 g) were mixed with hydrofluoric acid (20 mL) and continuously stirred at 35 °C for 72 h to selective removing of aluminum layers. After that, the mixture was washed with distilled water over and over again to make the final supernatant nearly neutral. The precipitate was dispersed in distilled water by sonication in a nitrogen atmosphere for 2 h in an ice-water bath. Finally, Ti_3C_2 nanosheets were obtained by freeze drying under vacuum for 3 days to sublimate the frozen solvent.

1.3 Exfoliation of Ti_3AlC_2

Ti_3AlC_2 powders (0.5 g) were mixed with hydrofluoric acid (20 mL) and continuously stirred at 35 °C for 72 hours to selectively remove the aluminum layers. Subsequently, the mixture was washed with distilled water until the final supernatant reached a nearly neutral pH. The resulting precipitate was dispersed in distilled water by sonication in a nitrogen atmosphere for 2 hours in an ice-water bath. Finally, $Ti_3C_2T_x$ nanosheets were obtained through freeze drying under vacuum for 3 days to sublime the frozen solvent.

1.4 Synthesis of $Ti_3C_2T_x$/ZIF-67

Typically, 50 mg of $Ti_3C_2T_x$ powders were dispersed in 15 mL of methanol. 1 mmol of $Co(NO_3)_2 \cdot 6H_2O$ was added to 15 mL of methanol to form solution. As followed, the $Co(NO_3)_2 \cdot 6H_2O$ solution was slowly added to the $Ti_3C_2T_x$ dispersion by ultrasonication for 10 min. 4 mmol of 2-methylimidazole was dissolved in 15 mL of methanol and the 2-methylimidazole solution was poured into the above $Ti_3C_2T_x$ /Co^{2+} dispersion. Then the mixed solution was aged for 24 h at room temperature, and the resulting precipitate was centrifuged

several times at 8000 rpm min^{-1}. At last, the final products were dried in vacuum.

1.5 Synthesis of $Ti_3C_2T_x$-Co@NCNTs

$Ti_3C_2T_x$/ZIF-67 powders and dicyandiamide were put at two separated porcelain boats and the boat for dicyandiamide was placed at the upstream side of the tube furnace. They were firstly heated at 430 ℃ for 8 h and then heated at 700 ℃ for 4 h (heating rate: 5 ℃/min) in under Ar atmosphere. The mass ratio of $Ti_3C_2T_x$/ZIF-67 and dicyandiamide is 1 : 20. The $Ti_3C_2T_x$-Co@NCNTs powders were harvested after cooling down to ambient temperature under Ar.

1.6 Synthesis of $Ti_3C_2T_x/CoS_2$@NCNTs, $Ti_3C_2T_x/CoSe_2$@NCNTs

$Ti_3C_2T_x$/Co@NCNTs powders and sulfur or selenium powders were put at two separated porcelain boats. They were heated to 650 ℃ and reacted for 2 h under argon (Ar) atmosphere. The mass ratio of $Ti_3C_2T_x$/Co@NCNTs to sulfur/selenium powder is 1 : 2.

1.7 Preparation of potassium Prussian blue (KPB).

KPB ($K_{0.22}Fe[Fe(CN)_6]_{0.805}$•$4.01H_2O$) was synthesized via a reported method. In the typical procedure, $K_4Fe(CN)_6$ (1 mmol) was added into deionized water (160 mL) with stirring for 2 h to prepare solution A. $FeCl_3$ (2 mmol) was added into deionized water (40 mL) to form solution B. Then, Solution B was slowly dissolved in solution A under stirring for 3 h and further aged for 24 h. The precipitates were retained via centrifugation, washing with DI-water and ethanol, and drying at 60 °C for 12 h in the vacuum oven.

1.8 Materials characterization

Scanning electron microscopy (SEM) was performed with a field-emission scanning electron microscope (Hitachi SU-8010, Japan) operated at a deceleration voltage of 1.5 kV to characterize the morphologies of the products. Transmission electron microscopy (TEM) images were taken with a JEOL JEM-2010 LaB6 high-resolution transmission electron microscope operated at 200 kV. High-resolution (HRTEM) images were taken with a JEOL JEM-2100F field-emission high-resolution transmission electron microscope operated at 200 kV. X-ray diffraction (XRD) patterns were recorded with a D8 Advance X-ray diffractometer (Bruker AXS company, Germany) equipped with a Cu-Kα radiation source (λ=1.5406 Å). Fourier transform infrared (FT-IR) spectra (Nicolet 5700, USA) of the samples were recorded using the KBr pellet method. A DXR Raman confocal microscope (Thermo Fisher Scientific, USA) with a 532 nm @10 mW Laser was used to record Raman spectra. X-ray photoelectron spectroscopy (XPS) measurements (VG Multilab 2000

photoelectron spectrometer) was performed with a Al Kα radiation as the excitation source under a 2×10^{-6} Pa vacuum; the C 1s peak of the surface adventitious carbon at 284.6 eV was used to calibrate all of the binding energies.

1.9 Electrolyte Preparation

The electrolyte system including 4 M KFSI (DME), 1 M KFSI(DME), 0.8 M KPF_6 (EC+DEC), 1 M KFSI (EC+DEC) were prepared by dissolving a certain amount of potassium salt (KFSI, KPF_6) into different solvents, including carbonate-based solvents (EC+DEC, 1 : 1 volume ratio), and ether-based solvents (DME) in an argon-filled glove box (O_2 < 0.1 ppm, H_2O < 0.1 ppm).

1.10 Electrochemical Characterization

The electrochemical tests were carried out using CR2032 coin-type cells. The working electrodes were prepared by mixing the active materials, Ketjen black, and polyvinylidene fluoride (PVDF), at a weight ratio of 70 : 20 : 10, which was then pasted on a copper foil. For half PIBs, K metal was used as the counter and reference electrode, and a polypropylene membrane (Celgard 2400) was used as the separator. Cell assembly was performed in an argon-filled glovebox. The mass loading of active material in the working electrode was about 0.8-1.0 mg cm^{-2}, and the diameter of the working electrode was 8 mm. The amount of electrolyte for each coin battery is around 240 μL. The charge and discharge tests were conducted with a NEWARE battery tester. Cyclic voltammograms (CVs) in a voltage range of 0.01-3 V and electrochemical impedance spectroscopy (EIS) spectrum were performed with an electrochemical workstation (IviumStath., Ivium Holland, Inc.). Electrochemical impedance spectra were obtained in the frequency range of 100 kHz-0.01 Hz with an amplitude of 5 mV. Galvanostatic intermittent titration technique (GITT) tests were recorded with a NEWARE battery tester in the potential range of 0.01-3 V at ambient temperature. After 20 charge-discharge cycles, GITT measurements were carried out at a low current density of 50 mA/g for 0.5 h followed by a rest interval of 2 h. For the construction of a flexible full battery, the KPB was utilized as cathode, and $Ti_3C_2T_x$-Co@NCNTs was served as anode with the same electrolyte and separator as in half battery. To form stable SEI films, the $Ti_3C_2T_x$-Co@NCNTs anode was first cycled at 50 A g^{-1} for 5 cycles between 0.01-2.6 V in half battery. KPB mixed with Ketjen black and PVDF (in a weight ratio of 70: 20: 10) were coated on Al foil. To eliminate the irreversible capacity, the KPB cathode was charged/discharged in the voltage of 2.5-4.0 V at 0.5 A g^{-1} for 5 cycles in half battery. In order to assure the suitable cathode to anode capacity for battery balance, the mass ratio of KPB to $Ti_3C_2T_x$-Co@NCNTs was maintained at 3 : 1 for a cathode capacity-limited configuration. To ensure that the KPB cathode is fully charged and discharged, the charging cut-off voltage

of the KPB cathode was 4.0 V and the corresponding $Ti_3C_2T_x$-Co@NCNTs anode discharge potential was 0.17 V. During the reverse process of the full-battery, the discharging cut-off voltage of the KPB cathode was 2.5 V and the corresponding $Ti_3C_2T_x$-Co@NCNTs anode charge potential was 1.6 V. Thus, the electrochemical performances of $Ti_3C_2T_x$-Co@NCNTs//KPB full battery were tested by galvanostatic charge/discharge in the voltage of 0.9-3.83 V.

1.11 Full potassium-ion battery

To prepare $K_{0.72}Fe[Fe(CN)_6]$ (PB) electrode, a slurry was first prepared by distributing $K_{0.22}Fe[Fe(CN)_6]$ precursor, Ketjen black, and polyvinylidene fluoride (PVDF) in N-methyl-2-pyrrolidone (NMP) solvent with a weight ratio of 70 : 20 : 10. Then the slurry was coated on Al foil and dried at 80 ℃ for 12 h. Subsequently, a half PIB was assembled with 3 M of KFSI in ethylene carbonate (EC)/dimethyl carbonate (DEC) (1:1, v/v) as electrolyte, K as counter electrode and the above coated $K_{0.22}Fe[Fe(CN)_6]$ as working electrode. The half-cell was finally discharged to 2 V to obtain $K_{0.72}Fe[Fe(CN)_6]$ cathode. For a full PIB, it was assembled with $Ti_3C_2T_x$ as anode, 3 M of KFSI in EC/DEC (1:1, v/v) as electrolyte and KPB as cathode. The mass ratio of anode and cathode is 1.0 : 1.05. The amount of electrolyte for each coin battery is around 150 μL for both half-cell and full-cell.

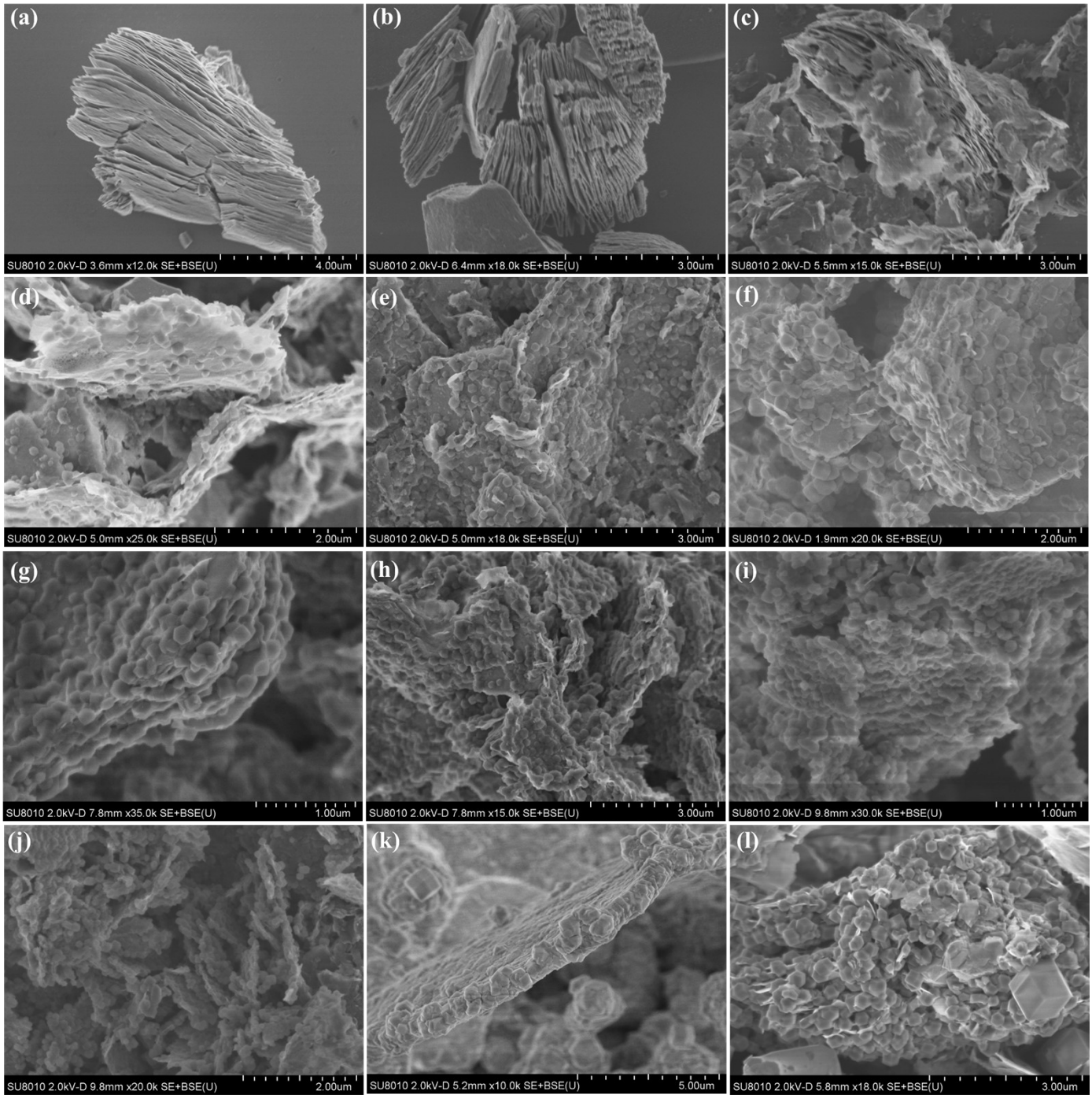

Figure S1: SEM images of (a-b) $Ti_3C_2T_x$, (c) the exfoliated $Ti_3C_2T_x$, (d-f) $Ti_3C_2T_x$/ZIF-67-0.5, (g-i) $Ti_3C_2T_x$/ZIF-67, (j-l) $Ti_3C_2T_x$/ZIF-67-2.

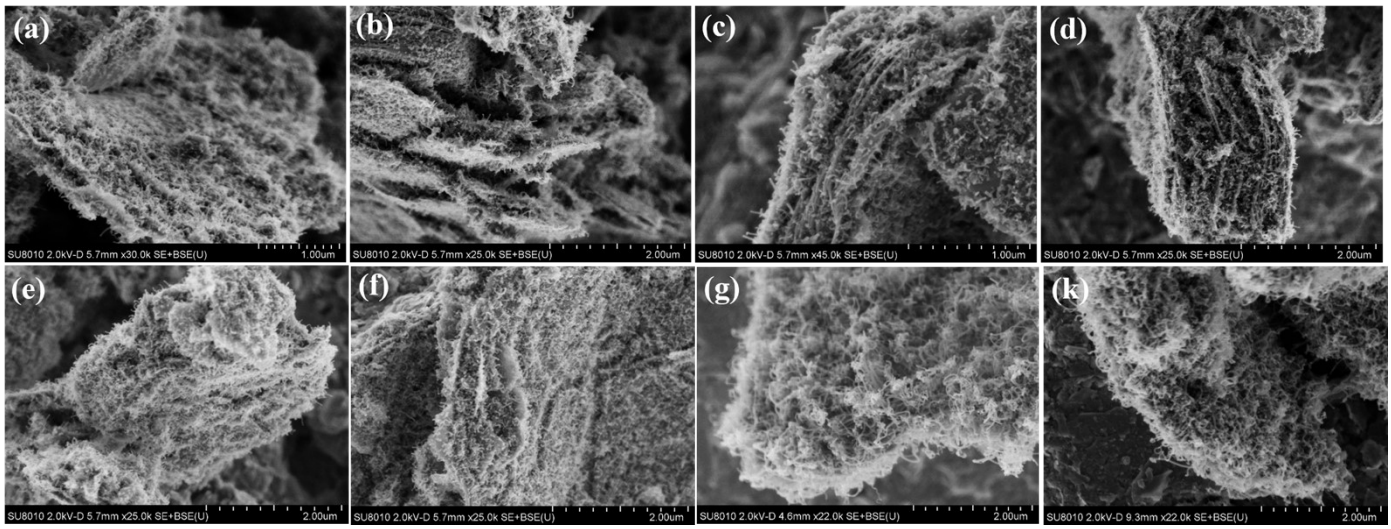

Figure S2: SEM images of $Ti_3C_2T_x$-Co@NCNTs hybrids.

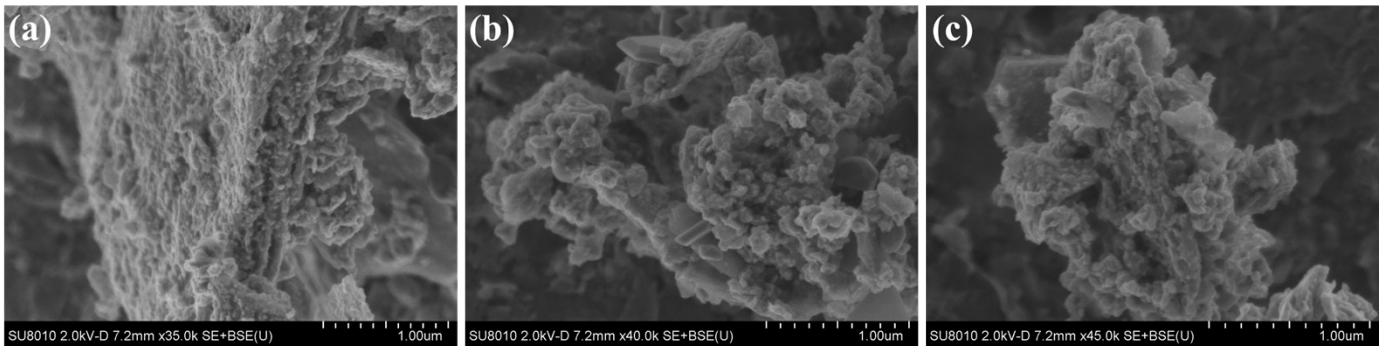

Figure S3: SEM images of $Ti_3C_2T_x$-Co@NC hybrids.

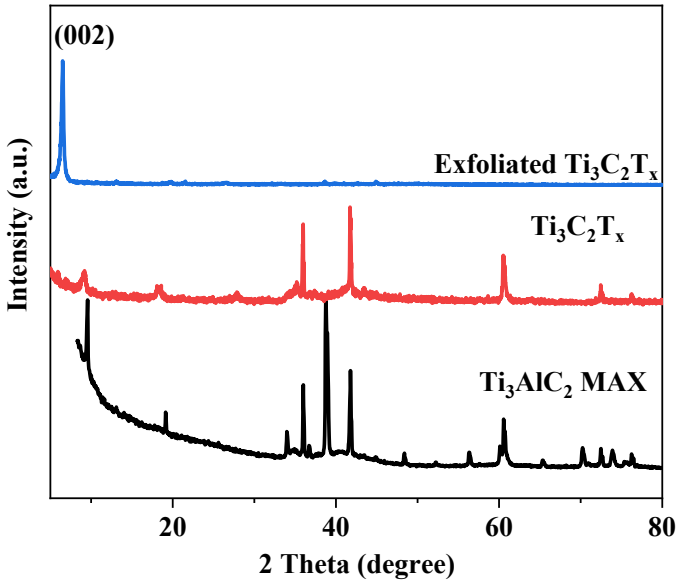

Figure S4: XRD patterns of MAX and $Ti_3C_2T_x$.

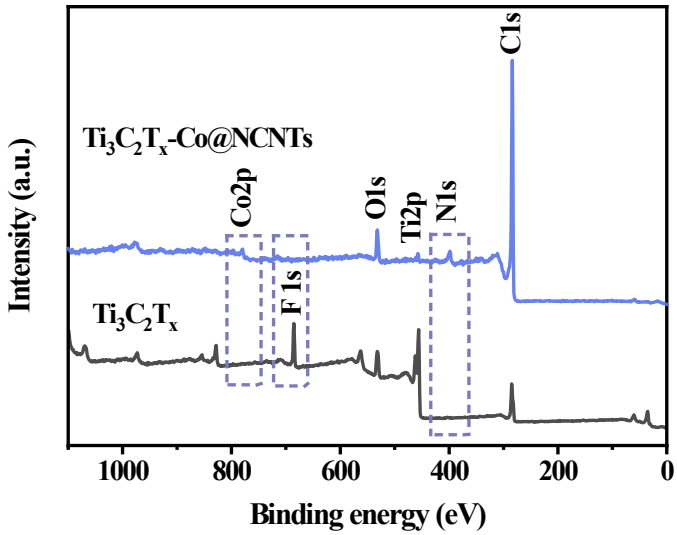

Figure S5: XPS survey of $Ti_3C_2T_x$ and $Ti_3C_2T_x$-Co@NCNTs.

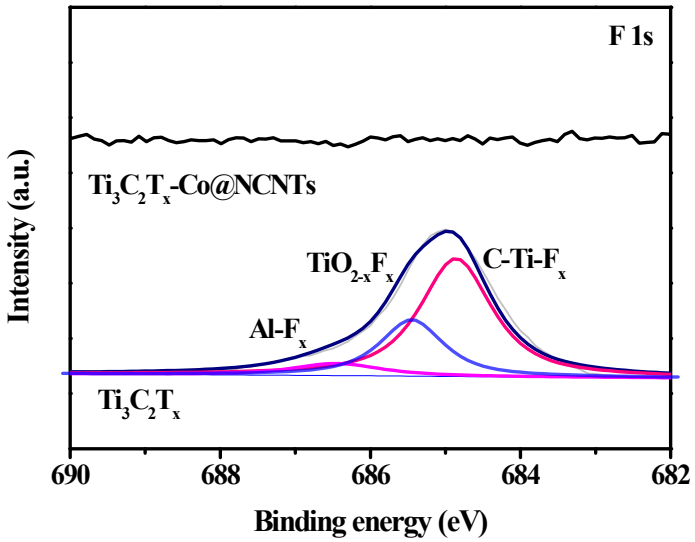

Figure S6: High-resolution XPS spectra of F 1s in $Ti_3C_2T_x$ and $Ti_3C_2T_x$-Co@NCNTs.

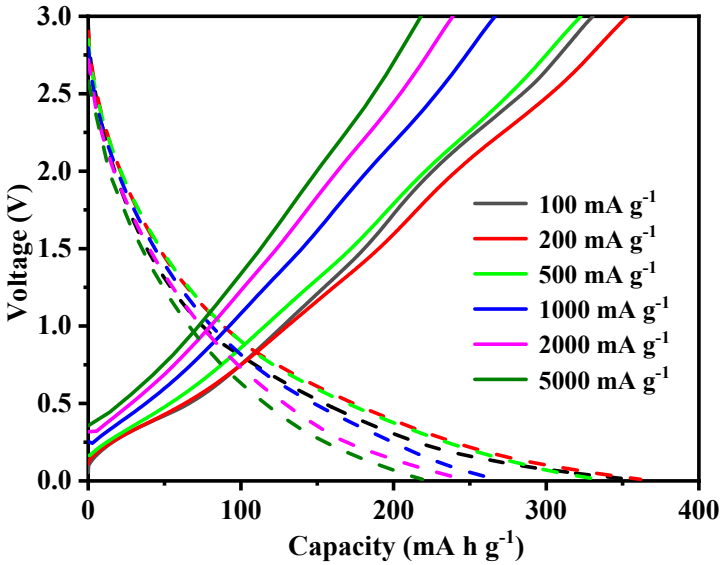

Figure S7: GDV curves of $Ti_3C_2T_x$-Co@NCNTs in 1 M KFSI (DME) at different current densities.

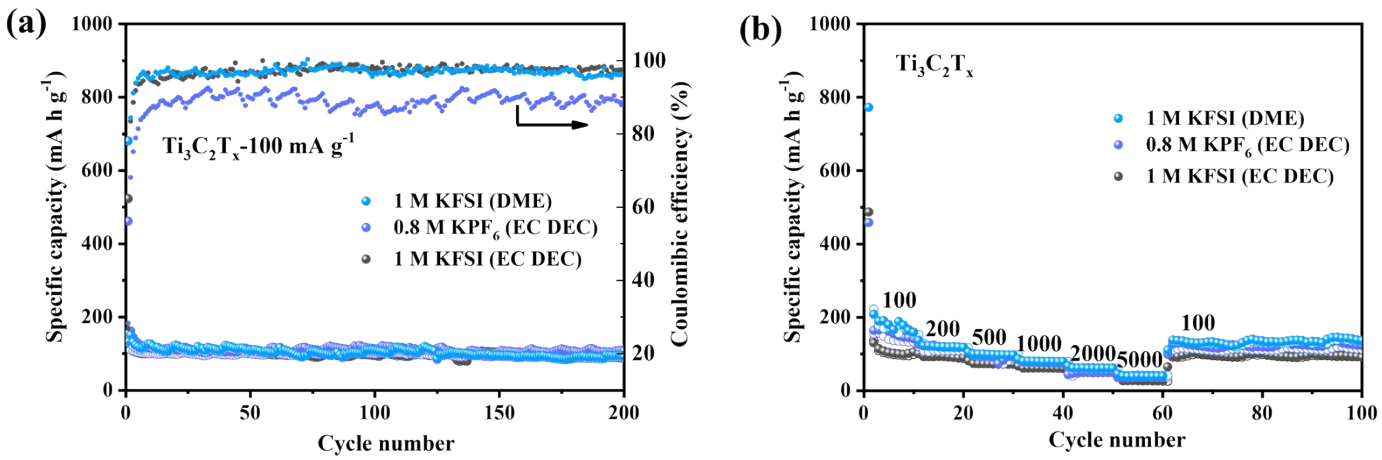

Figure S8: (a) Cycling performance of the as-prepared $Ti_3C_2T_x$ electrode at the current density of 100 mA g^{-1}. (b) Rate performance of $Ti_3C_2T_x$ electrode at various current densities from 100 to 5000 mA g^{-1} in 1 M KFSI (DME), 0.8 M KPF_6 (EC/DEC) and 1 M KFSI (EC/DEC).

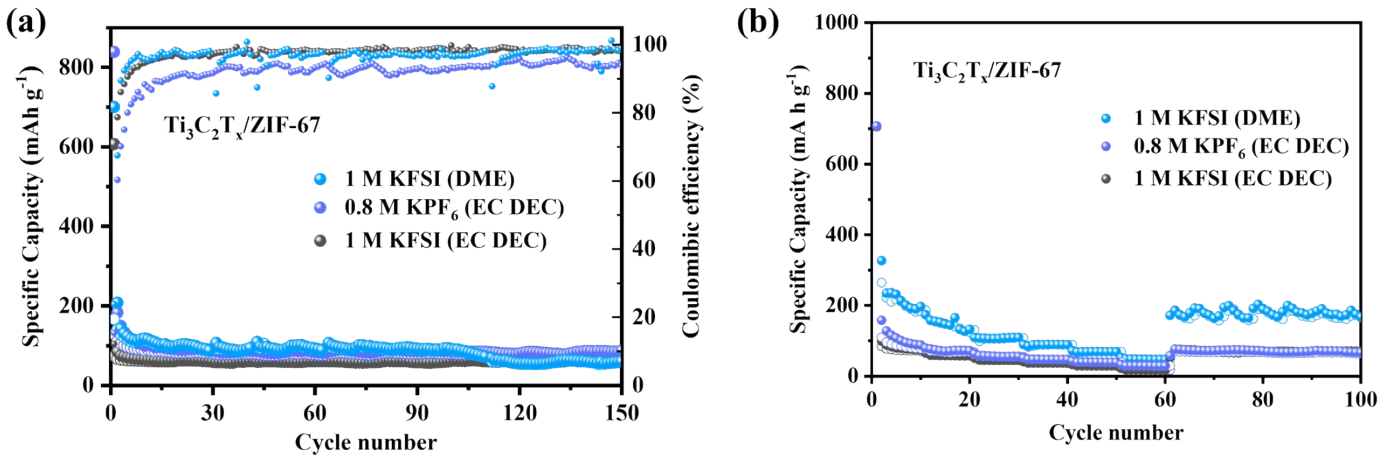

Figure S9: (a) Cycling performance of the as-prepared $Ti_3C_2T_x$/ZIF-67 electrode at the current density of 100 mA g^{-1}. (b) Rate performance of $Ti_3C_2T_x$/ZIF-67 electrode at various current densities from 100 to 5000 mA g^{-1} in 1 M KFSI (DME), 0.8 M KPF_6 (EC/DEC) and 1 M KFSI (EC/DEC).

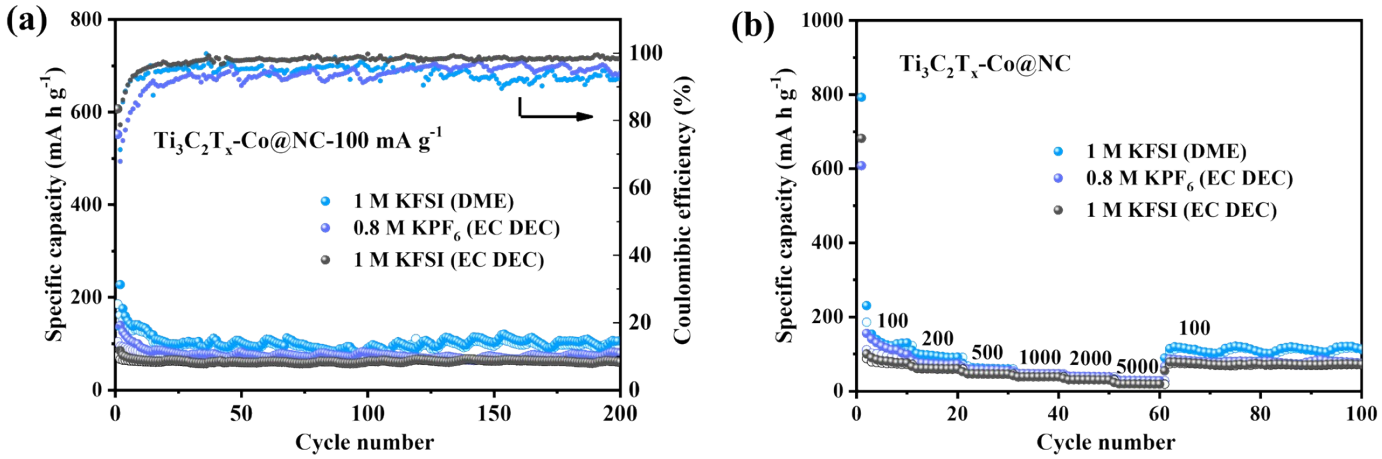

Figure S10: (a) Cycling performance of the as-prepared $Ti_3C_2T_x$-Co@NC electrode at the current density of 100 mA g^{-1}. (b) Rate performance of $Ti_3C_2T_x$ electrode at various current densities from 100 to 5000 mA g^{-1} in 1 M KFSI (DME), 0.8 M KPF_6 (EC/DEC) and 1 M KFSI (EC/DEC).

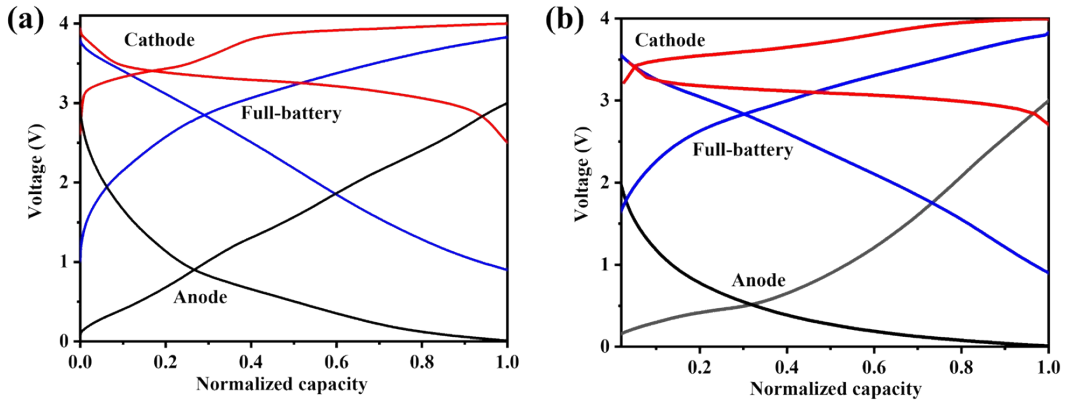

Figure S11: GDV curves of $Ti_3C_2T_x$-Co@NCNTs in (a) 1 M KFSI (DME), and (b) 0.8 M KPF_6 (EC/DEC) for full-cell.

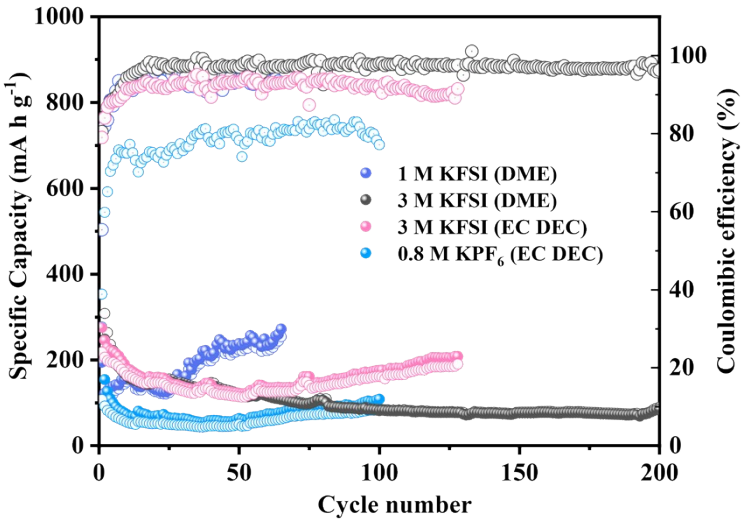

Figure S12: The cycling performance of full cell at 100 mA g^{-1} in 3 M KFSI (DME) and 0.8 M KPF_6 (EC/DEC).

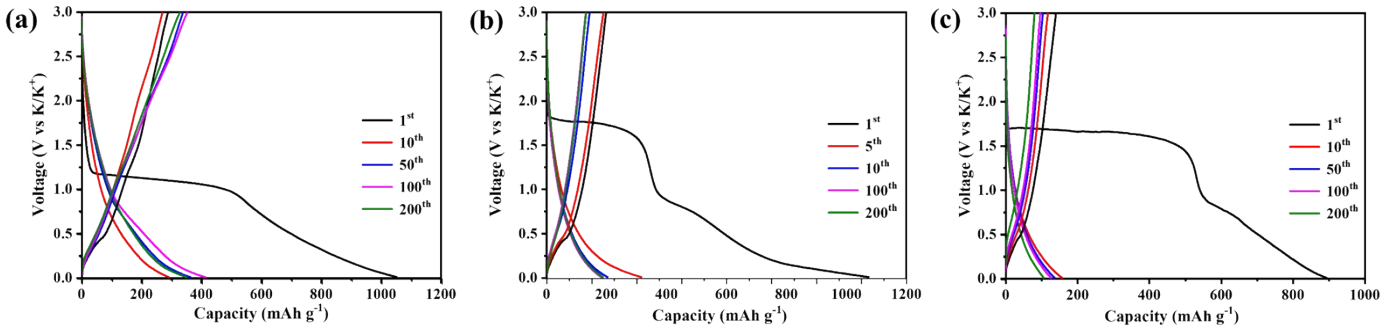

Figure S13: GDV curves of $Ti_3C_2T_x$-Co@NCNTs in (a) 1 M KFSI (DME), (b) 0.8 M KPF_6 (EC/DEC) and (c) 1 M KFSI (EC/DEC) at 100 mA g^{-1}.

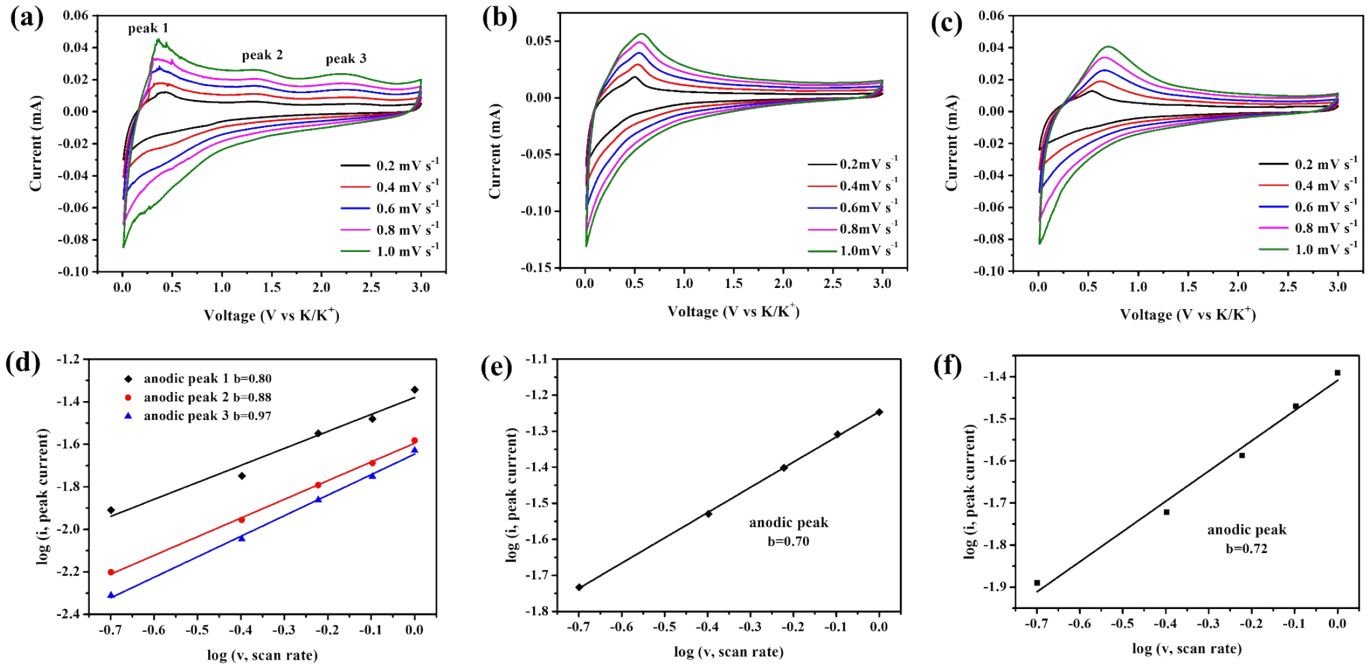

Figure S14: CV curves of $Ti_3C_2T_x$-Co@NCNTs at different scan rates in (a) 1 M KFSI (DME), (b) 0.8 M KPF_6 (EC/DEC) and (c) 1 M KFSI (EC/DEC).

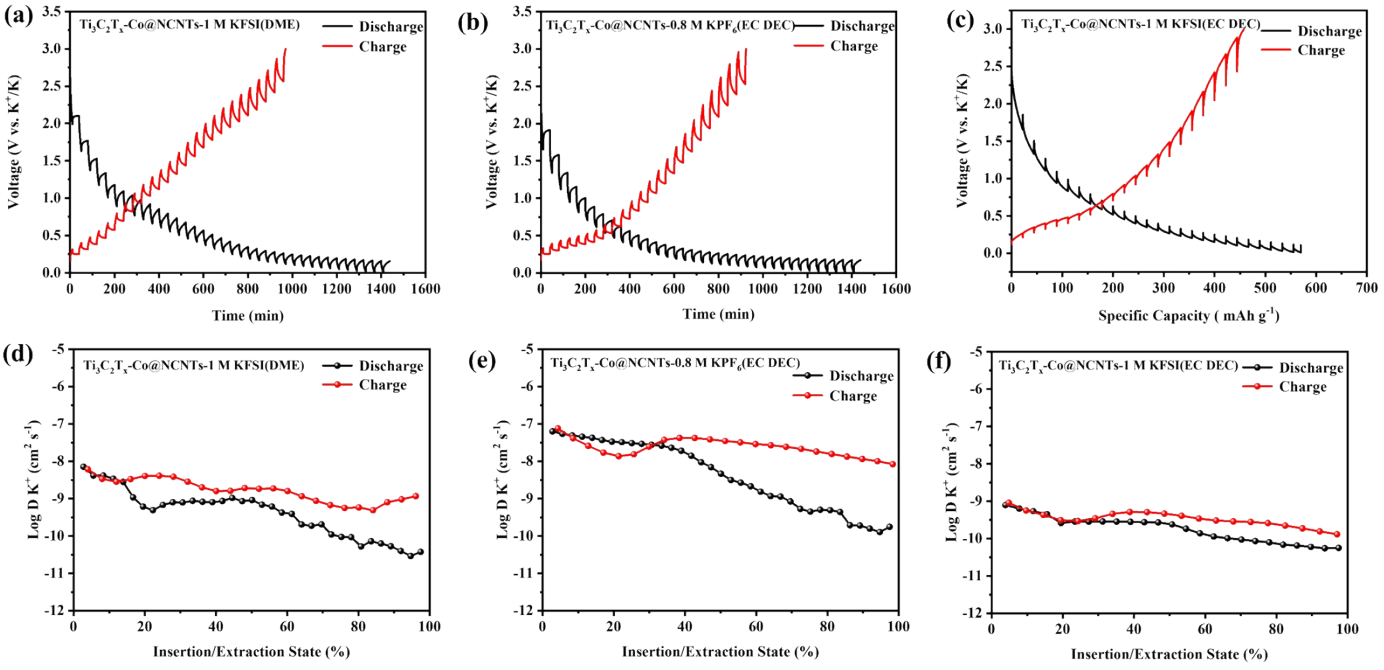

Figure S15: (a-c) GITT curves and (d-f) the calculated D_k values from GITT in different electrolyte system.

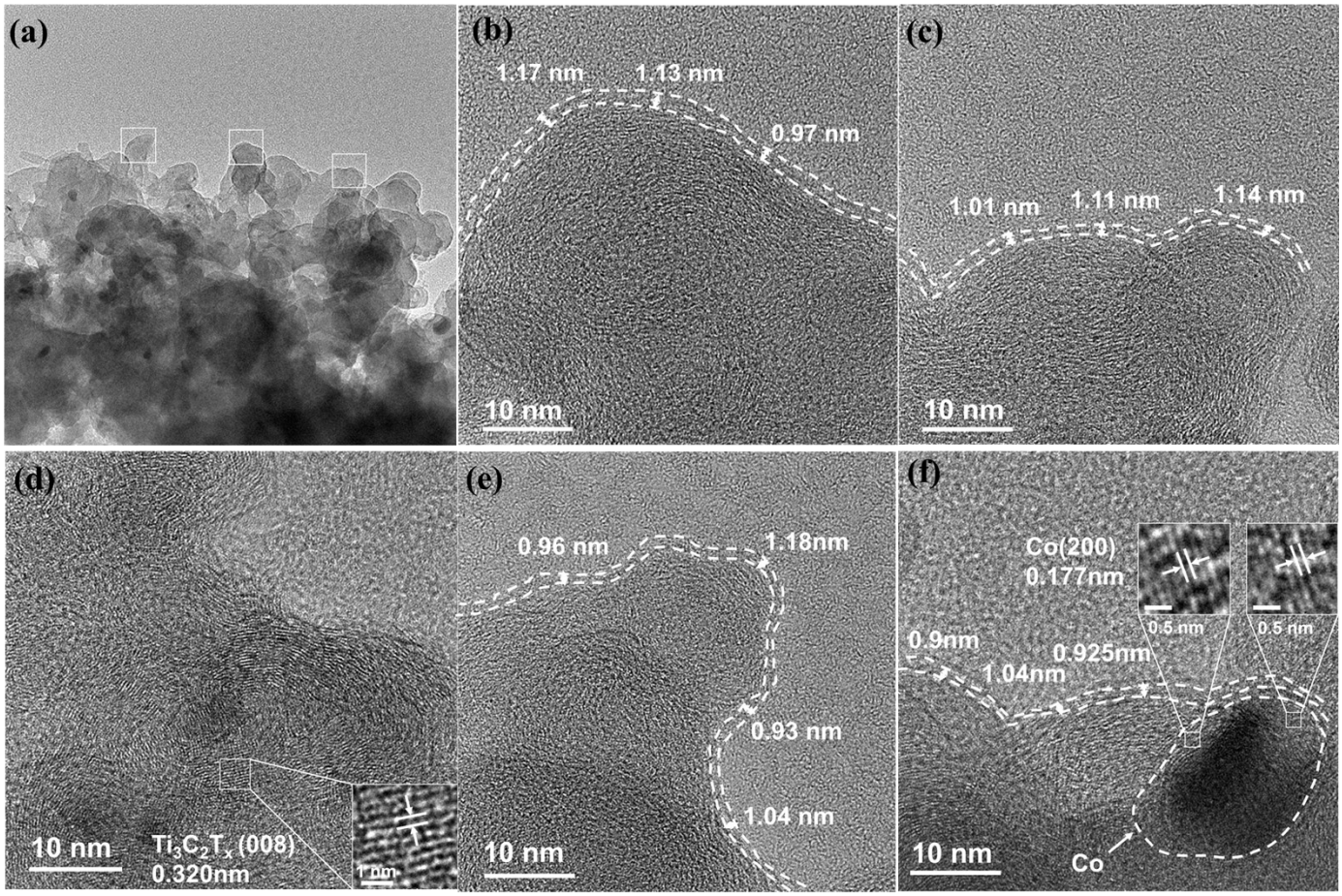

Figure S16: SEI layers of $Ti_3C_2T_x$-Co@NCNTs in 1 M KFSI (DME).

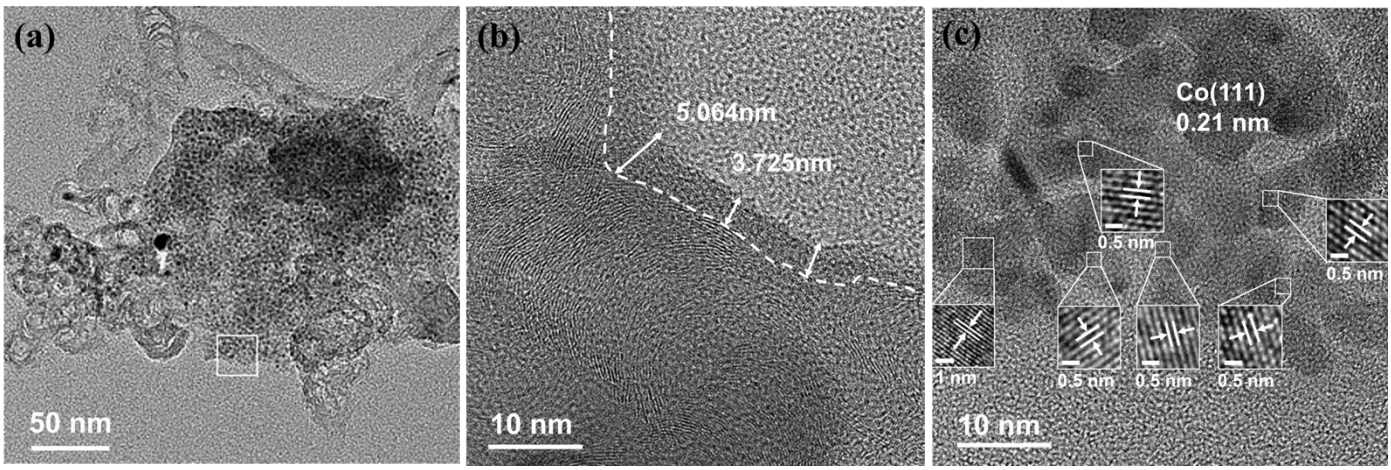

Figure S17: SEI layers of $Ti_3C_2T_x$-Co@NCNTs in 0.8 M KPF_6 (EC DEC).

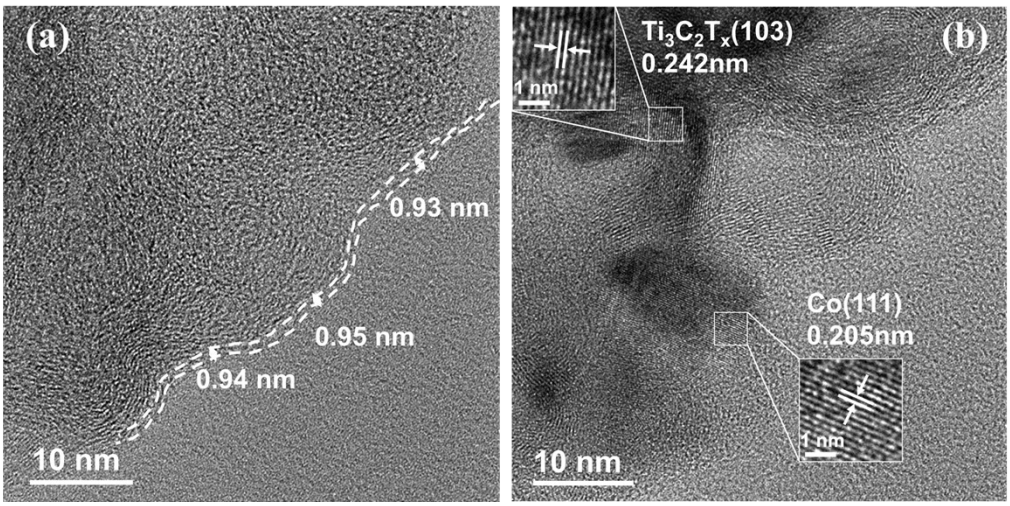

Figure S18: SEI layers of $Ti_3C_2T_x$-Co@NCNTs in 1 M KFSI (EC DEC).

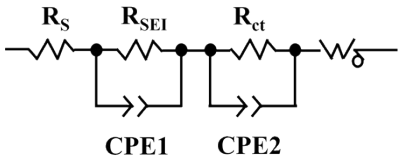

Figure S19: The equivalent circuit diagram for EIS data.

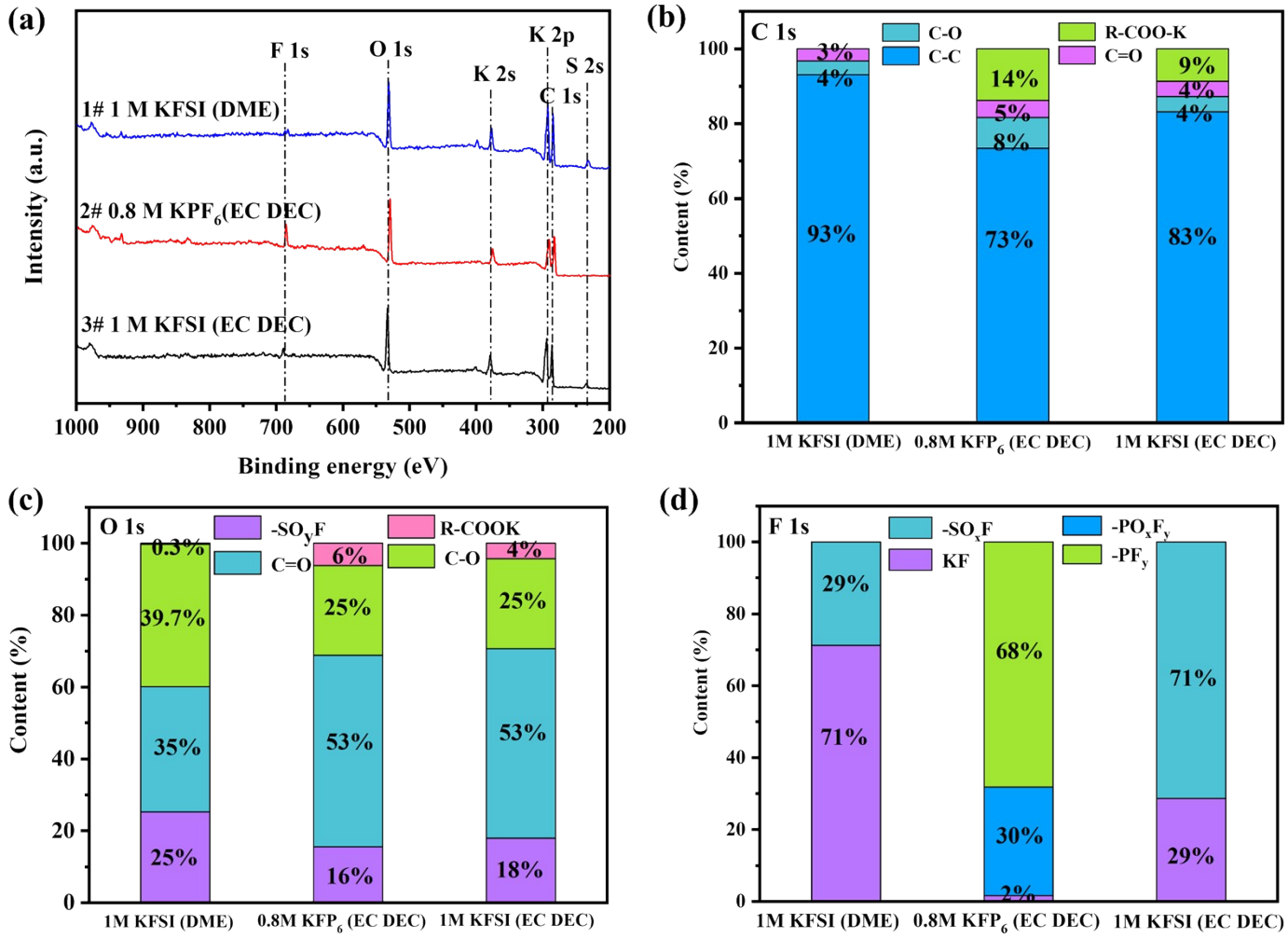

Figure S20: (a) full-scale XPS survey, and (b-d) SEI species ratio.